analytical chemistry

ARTICLE

pubs.acs.org/ac

Use of Real-Time, Label-Free Analysis in Revealing Low-Affinity Binding to Blood Group Antigens by *Helicobacter pylori*

Y. Y. Fei,[†] A. Schmidt,[⊥] G. Bylund,[⊥] D. X. Johansson,[∥] S. Henriksson,[∥] C. Lebrilla,[§] J. V. Solnick,[‡] T. Borén,[*,∥,⊥] and X. D. Zhu[*,†]

[†]Department of Physics, [‡]Departments of Medicine and Microbiology and Immunology, Center for Comparative Medicine, and [§]Department of Chemistry, University of California, Davis, Davis, California 95616, United States

[∥]Department of Medical Biochemistry and Biophysics, Umeå University, SE-90187 Umeå, Sweden

[⊥]Helicure AB, c/o Umeå Biotech Incubator, Box 7997, Umeå, Sweden

Supporting Information

ABSTRACT: Infectious diseases are often initiated by microbial adherence that is mediated by the binding of attachment molecules, termed adhesins, to cell surface receptors on host cells. We present an experimental system, oblique-incidence reflectivity difference (OI-RD) microscopy, which allows the detection of novel, low-affinity microbial attachment mechanisms that may be essential for infectious processes. OI-RD microscopy was used to analyze direct binding of the oncopathogen, *Helicobacter pylori* (*H. pylori*) to immobilized glycoconjugates in real time with no need for labeling tags. The results suggest the presence of additional Lewis b blood group antigen (Le^b) binding adhesins that have not been detected previously. OI-RD microscopy also confirmed the high-affinity binding of *H. pylori* outer-membrane protein BabA to Le^b. The OI-RD microscopy method is broadly applicable to real-time characterization of intact microbial binding to host receptors and offers new strategies to elucidate the molecular interactions of infectious agents with human host cells.

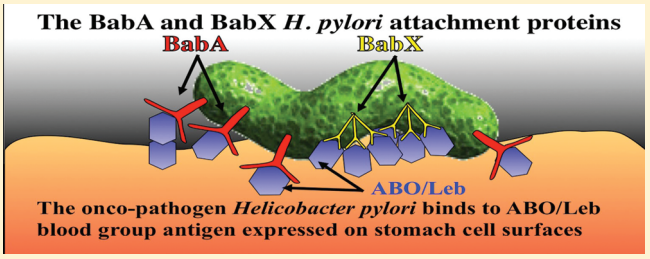

The first step in the pathogenesis of a mucosal infectious agent is typically adherence mediated by the binding of microbial attachment proteins to specific host cell surface carbohydrates. Examples include binding of adhesins on the influenza virus to sialylated carbohydrates on a host cell surface and binding by the G-adhesin of P-fimbriated *Escherichia coli* to the P blood group antigens in urinary tract epithelium. Methods that detect the specific binding of microbial adhesins to host glycans have the potential to enhance our understanding of microbial pathogenesis and may lead to translational applications to prevent or treat infectious diseases.

Carbohydrate microarrays are used to probe putative glycan binding proteins, yet few have been used to examine the binding properties of intact microbes. Moreover, standard microarray methods utilize affinity tags and fluorescent labels for detection; these alter the microbial interaction with glycans,[1,2] often in unknown ways. Oblique-incidence reflectivity difference (OI-RD) scanning microscopy (Figure 1) is a recently developed method for the analysis of label-free biomolecular binding to immobilized targets.[3−9] OI-RD microscopy measures small changes in the phase and amplitude of a reflected optical wave from a solid surface due to the reaction of a solution-phase probe (in this study, microbial cells and adhesins) with target molecules (here, immobilized glycans). OI-RD microscopy has been utilized successfully in several biomolecular binding assays, including DNA hybridization,[3] antigen−antibody interactions,[5−8] and screens of small-molecule libraries for protein ligands.[9]

A novel application of OI-RD microscopy is real-time analysis of whole bacterial cell binding to surface-presented cognate host cell receptors; here we used OI-RD microscopy to analyze the binding of *Helicobacter pylori*, which is the major cause of peptic ulcer disease and gastric cancer[10] to carbohydrate receptors. *H. pylori* attachment to the gastric epithelium is mediated in part by the blood group antigen binding adhesin (BabA), which binds with high affinity to the fucosylated ABO blood group antigens and in particular to the Lewis b antigen (Le^b) of blood group O. Although the ABO blood group system is based on expression of the ABO antigens on erythrocytes, primary expression of these antigens is on the gastrointestinal epithelium.[11,12] In this study, OI-RD microscopy confirmed that wild-type *H. pylori* binds specifically to Le^b but not to other fucosylated antigens such as Le^a, Le^x, or Le^y. Since BabA is a member of a large family of *H. pylori* outer-membrane proteins (OMPs),[13] there are likely additional, unrecognized adhesins with affinity for other glycans expressed on the gastric epithelium. Indeed, OI-RD analysis demonstrated that *H. pylori* mutants that lack BabA still bind

Received: May 17, 2011
Accepted: July 1, 2011

   dx.doi.org/10.1021/ac201260c | *Anal. Chem.* XXXX, XXX, 000–000

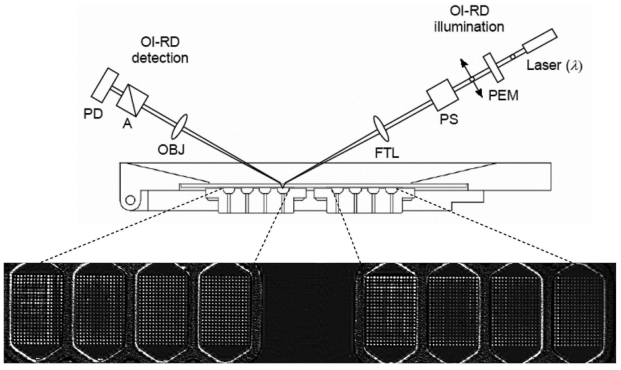

Figure 1. Oblique-incidence reflectivity difference (OI-RD) scanning microscope equipped with a combination of a *y*-scan mirror and an *x*-scan linear stage. A 1 in. × 3 in. glass slide printed with eight microarrays, each over an area of 3 mm × 4.5 mm, was assembled with a fluidic system with eight chambers, each of which contained a microarray (A). The fluidic system was mounted on the *x*-scan linear stage. PEM: photoelastic modulator. PS: phase shifter. FTL: encoded scan mirror for *y*-scan. OBJ: objective lens. A: polarization analyzer. PD: photodiode detector. The OI-RD image displays eight protein microarrays, each comprising 315 bovine serum albumin (BSA) spots (see the Supporting Information, text S1).

specifically to Le^b, albeit with lower binding strength. Hence, OI-RD microscopy not only confirmed the established BabA-mediated binding to Le^b, but also revealed the presence of a novel Le^b binding mechanism. These results demonstrate that OI-RD microscopy is generally applicable to real-time characterization of both high- and low-affinity microbial binding to host receptors and offers a novel methodology to better investigate and understand microbial cell attachment to human host cells.

MATERIALS AND METHODS

Microarray of Lewis Glycoconjugates. Lewis glycans, Le^a−HSA, Le^b−HSA, Le^x−HSA, and Le^y−HSA (Isosep AB; Tullinge, Sweden), were covalently attached to human serum albumin (HSA) at molar ratios of approximately 20 glycans and dispensed in a 384-well plate (Genetix, Charlestown, MA) in concentrations of 2, 4, 8, and 16 μM. The glycoconjugate solutions were spotted into a microarray using an OmniGrid100 contact-printing arrayer (Digilab, Holliston, MA). The microarray consisted of nine replicates of Lewis glycoconjugates at each concentration (in the form of a 3 × 3 lattice), plus two rows of control spots (12 each) printed from 8 μM bovine serum albumin (BSA, Jackson ImmunoResearch Laboratories, PA). A total of 144 target spots and 24 control spots cover a footprint of 3 mm ×4.5 mm. The average diameter of the printed spots is 100 μm, and the center-to-center spacing between the neighboring spots is 300 μm. The printed glycoconjugates were bound covalently to the glass slide by the exothermic reaction of amine residues on HSA and BSA with epoxy groups on the glass surface. Eight glycoconjugate microarrays were printed in separate locations on one 1 in. × 3 in. glass slide (see the Supporting Information, Figure S1).

The slide was assembled with a fluidic system with each of the eight printed microarrays housed in a separate chamber (volume/chamber, 30 μL) as illustrated in Figure 1. Before reaction, the printed side of the slide was washed with 2 mL of 1× phosphate-buffered saline (PBS) at flow rate of 5 mL/min.

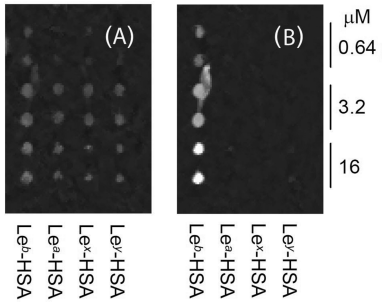

Figure 2. Recombinant BabA protein binds specifically to Le^b antigen. (A) The OI-RD image of a printed Lewis antigen microarray (Le^b, Le^a, Le^x, Le^y) with all glycoconjugates visualized before incubation with recombinant $BabA_{547}$. Each glycoconjugate was printed twice at three target concentrations. (B) Recombinant $BabA_{547}$ binds to Le^b−HSA but does not bind to the closely related Lewis antigens.

The washed surface was then exposed to the BSA solution for 30 min and washed again with 2 mL of 1× PBS at 5 mL/min. The blocked microarray surface was imaged again with the OI-RD microscope prior to reaction.

Recombinant BabA. A truncated, soluble BabA derivative lacking a predicted C-terminal β-barrel structure,[13] designated $BabA_{547}$, was expressed in *E. coli* with a periplasmatic leader sequence (see the Supporting Information, text S3). Specific binding of $BabA_{547}$ to Le^b was confirmed by enzyme-linked immunosorbent assay (ELISA) (see the Supporting Information, text S4 and Figure S3).

Binding Reaction of Recombinant BabA ($BabA_{547}$) with a Lewis Glycoconjugate Microarray. For $BabA_{547}$ binding assays, the four Lewis glycoconjugates were printed separately at concentrations of 0.64, 3.2, and 16 μM. Each target was printed twice for a total of 24 spots.

***H. pylori* Strains.** Wild-type (WT) *H. pylori* strains J166 and J99 were grown for 24 h on solid media[25] and harvested into blocking buffer (0.2% BSA, 0.05% Tween 20, and 0.05% sodium azide). The concentration was adjusted to an optical density of 0.10 at 600 nm. Isogenic deletions of *babA* (Δ*babA*) or both *babA* and *sabA* (Δ*babA*Δ*sabA*) were as described previously.[14,20] *H. pylori* CCUG 17875[20] was used to express recombinant BabA and to detect bacterial cells binding to Le^b by fluorescent microscopy.

Whole *H. pylori* Cell Binding Reaction with Lewis Glycoconjugate Microarrays. For the association phase, we replaced 1× PBS in the fluidic chamber with 0.2 mL of the bacterial solution at 5 mL/min and incubated at room temperature for 66 h. For the dissociation phase, we replaced the bacterial solution with 0.3 mL of 1× PBS at 5 mL/min and incubated for 28 h at room temperature. The long dissociation time is likely due to the presences of multiple adhesin molecules on the bacterial cell surface that bind to multiple receptors. Three bacterial strains were loaded simultaneously into six chambers, each with a glycoconjugate microarray. The microarray in one of the remaining two chambers was exposed only to 1× PBS as a control.

OI-RD Scanning Microscopy for Label-Free Detection of *H. pylori* Binding to Lewis Glycoconjugates. We measured the amount of recombinant BabA proteins and the bacteria captured by the Lewis glycoconjugates (per unit area) with the scanning OI-RD microscope as illustrated in Figure 1. The working principle of the microscope has been reported previously,[7,9] and the key features of the microscope used in the present study

dx.doi.org/10.1021/ac201260c |*Anal. Chem.* XXXX, XXX, 000–000

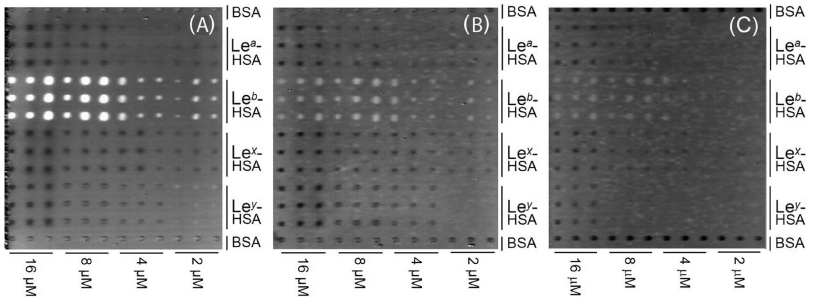

Figure 3. *H. pylori* binds to the Le^b antigen in a BabA-independent manner. (A) The J166WT strain, (B) the J166Δ*babA* deletion mutant strain, and (C) the J99Δ*babA* deletion mutant strain (F) were incubated for 66 h at room temperature on an extended Lewis glycoconjugate microarray (Le^b, Le^a, Le^x, Le^y, each at four target concentrations). The OI-RD images show that both the WT and the *babA* deletion mutants bind specifically to the Le^b antigen, although the WT strain has higher binding strength. The results were obtained by subtracting the images taken before incubation from the images taken after incubation.

are described in the Supporting Information (text S1.) Briefly, binding of bacterial cells causes changes in the phase and amplitude of an optical beam reflected from the surface of the solid support. These changes arise from differences in the refractive index of the target−probe layer, the solid support, and the aqueous ambient and depend on whether the optical beam is p-polarized or s-polarized. A scanning OI-RD microscope measures the differential reflection change between two polarizations across a microarray-covered solid surface.[4,7,9] To characterize a glycoconjugate microarray and its subsequent reaction with BabA protein, we measured the differential phase change (see the Supporting Information, text S1, eqs S2 and S3) for contrast. To characterize the *H. pylori* whole-cell binding reaction with a glycoconjugate microarray, we measured differential amplitude change (see the Supporting Information, text S1, eq S4) for contrast. The image of the glycoconjugate microarrays was acquired using a step size of 10 μm. By taking a sequence of optical images at 2 h time intervals, we obtained real-time binding curves as well as the end-points of the bacterial reactions.

RESULTS

Recombinant BabA Binds Specifically to Surface-Presented Le^b. We first used OI-RD to study the binding of recombinant BabA to a Lewis glycoconjugate microarray. Figure 2A shows the OI-RD image of a Lewis antigen glycoconjugate microarray before the experimental reaction, and Figure 2B shows the change in the image after the microarray was incubated with 400 μM recombinant $BabA_{547}$ for 60 min. Recombinant $BabA_{547}$ binds to Le^b but not to the related fucosylated antigens Le^a, Le^x, and Le^y. This observation supports the notion that binding of *H. pylori* to Le^b moieties on a host surface is mediated primarily by the affinity of the BabA adhesin for Le^b.

***H. pylori* Binds to Le^b in a BabA-Independent Manner.** We next investigated the binding of *H. pylori* strain J166 whole cells to the Lewis glycoconjugate microarray. As shown in Figure 3A, wild-type *H. pylori* J166 exhibits specific binding to Le^b, but not to Le^a, Le^x, Le^y, or to nonglycosylated BSA controls. Surprisingly, *H. pylori* J166Δ*babA*, which does not express BabA and does not bind to Le^b−HSA in solution, also exhibits specific binding to Le^b, although binding is reduced compared to binding of the wild-type J166 strain (Figure 3B). We observed a similar binding pattern for *H. pylori* strain J99 (Figure 3C). These observations suggest that the *H. pylori* strains have previously unrecognized BabA-independent Le^b-binding activity.

Quantitative Analysis Confirms BabA-Independent Binding to Le^b. We next quantified the bacterial binding by separating the optical signals due to bacterial binding to glycoconjugates from the signals due to nonspecific binding to the blocking agent, BSA. Even at the printing concentration of 16 μM, immobilized glycoconjugates do not fully cover the functionalized solid surface. Specifically, surface coverage of the glycoconjugate targets (Θ_{target}) is less than unity, and the remaining surface ($1 - \Theta_{target}$) is covered with the blocking agent, BSA. Thus, both the glycoconjugates and the blocking BSA on the surface contribute to the OI-RD signal shown in Figure 3. If we designate $S_{blocking\text{-}BSA}$ as the optical signal from the surface fully covered with BSA, and S_{target} as the signal from the surface fully covered with glycoconjugates (or printed BSA), the total optical signal S in Figure 3 is expressed as

$$S = \Theta_{target} S_{target} + (1 - \Theta_{target}) S_{blocking\text{-}BSA} \quad (1)$$

We determined Θ_{target} from the OI-RD microscopy images obtained before and after blocking with BSA (see the Supporting Information, text S2). With the information on Θ_{target} and $S_{blocking\text{-}BSA}$ from the unprinted surface region, we calculated S_{target} using eq 1 from the data shown in Figure 3. Parts A and B of Figure 4 show, respectively, the results for *H. pylori* J166 (WT) and J166Δ*babA* binding to the four Lewis glycoconjugates and printed BSA control. Wild-type J166 binds to Le^b with high strength and specificity, whereas the J166Δ*babA* mutant shows lower but still specific affinity for Le^b. The latter observation supports the notion that *H. pylori* J166 has both BabA-dependent and BabA-independent Le^b-binding adhesin activity. Findings were similar for *H. pylori* strain J99WT, which differs from J166 in that it in addition to BabA also expresses the sialyl-Le^x binding protein, SabA.[14] Both J99WT and the J99Δ*sabA* mutant bind to Le^b with high affinity and specificity, whereas the J99Δ*babA*Δ*sabA* and J99Δ*babA* mutants bind to Le^b with reduced but still specific affinity (Figure 4, parts C and D). These results suggest that, like J166, the J99 strain also has additional Le^b-binding activity due to one or more outer-membrane proteins. This complementary adhesin activity is specific for Le^b (Figure 4C) and is not associated with the SabA adhesin, since the Δ*sabA* mutants exhibit intact Le^b binding (Figure 4, parts C and D).

The detection sensitivity of the OI-RD microscopy technique was compared to that of conventional microscopy by applying

dx.doi.org/10.1021/ac201260c |*Anal. Chem.* XXXX, XXX, 000–000

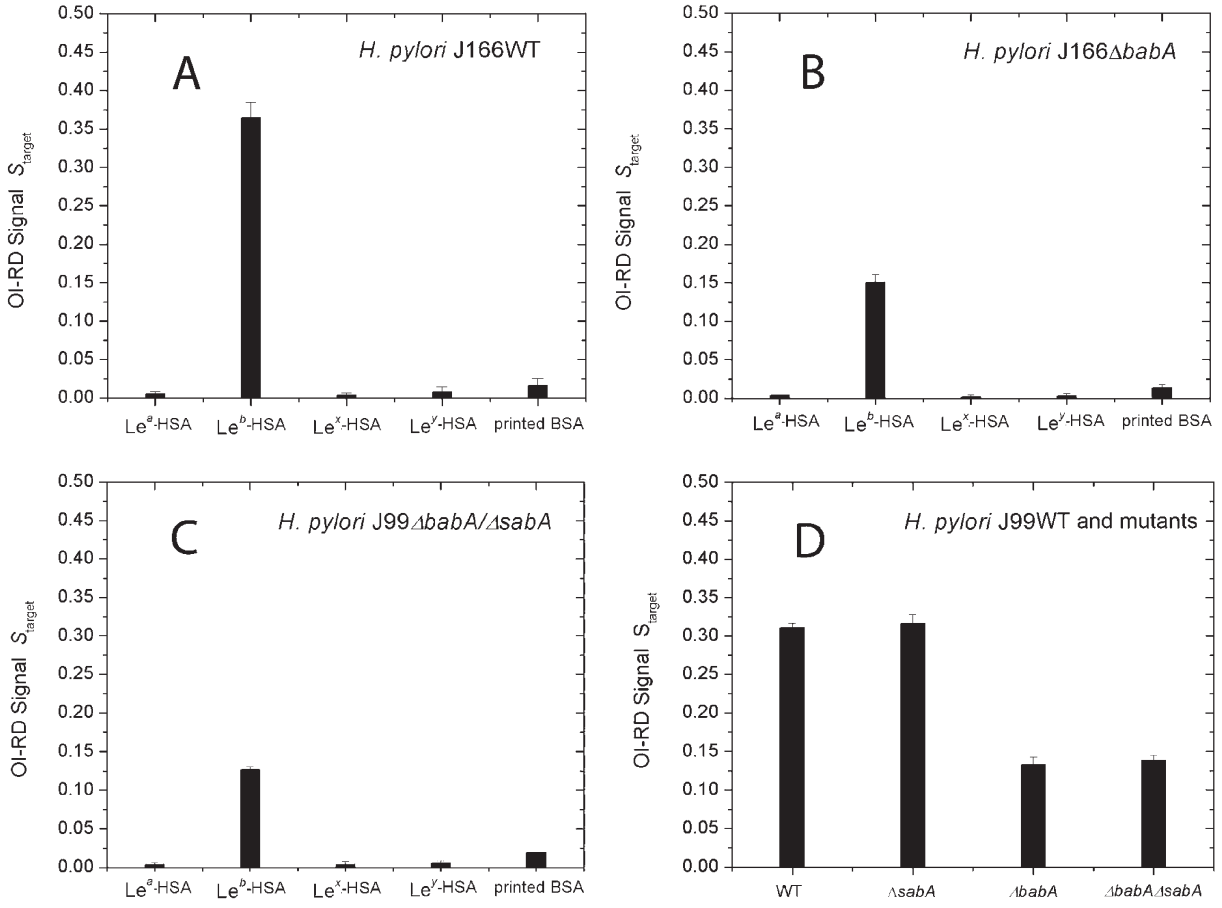

Figure 4. *H. pylori* binds to the Le^b antigen in a BabA- and SabA-independent manner. Binding of (A) J166WT cells (*babA* intact), (B) J166Δ*babA* cells (*babA* deleted), and (C) J99Δ*babA*/Δ*sabA* (*babA* and *sabA* deleted) cells to Lewis arrays as detected by OI-RD signals S_{target}. All three strains bind to Le^b, but they do not bind Le^a, Le^x, Le^y (albumin glycoconjugates), or to BSA printed on functionalized glass. (D) *H. pylori* binds more strongly to Le^b in the presence of BabA (in the J99WT strain and the J99Δ*sabA* deletion mutant), whereas the SabA adhesin does not contribute to *H. pylori* binding to Le^b.

fluorescently labeled *H. pylori* CCUG 17875 bacterial cells to a fresh Lewis glycoconjugate microarray (see the Supporting Information, Figure S2). In agreement with the OI-RD results (Figure 3A), *H. pylori* demonstrated strong binding affinity to immobilized Le^b, in the range of 400 bacterial cells over a single printed spot. Binding to other Lewis glycoconjugates, such as Le^y and Le^x, was close to background, although Le^a and the printed BSA control showed some residual binding. The latter implies a nonspecific interaction, which presumably relates to the use of the FITC tag on the fluorescent labeled bacterial cells.

Real-Time Analyses Demonstrate Slow Bacterial Binding Kinetics. The optical signals shown in Figures 3 and 4 were obtained after 66 h of incubation (before the dissociation phase). Using eq 1 and the images taken before and after that time, we obtained S_{target} as a function of time and constructed the association−dissociation curves of *H. pylori*−Le^b binding (Figure 5). At a bacterial concentration of 10^8 cells/mL ($[c]$ = 0.17 pM), the association of *H. pylori* J166 with immobilized Le^b took over 60 h to level off. The difference in association kinetics for J166 and the J166Δ*babA* mutant shows that the association rate is partly limited by mass transport of the bacteria to the microarray-covered solid surface and partly limited by association efficiency with the glycoconjugates. By fitting the association−dissociation curves, we found that K_d for the wild-type J166 to Le^b was 0.7×10^{-15} M, whereas K_d for the J166Δ*babA* mutant to Le^b was 9.2×10^{-15} M (weaker binder).

DISCUSSION

Microbial pathogens that infect mucosal surfaces must negotiate a delicate balance between intimate attachment to host epithelial cells and persistent access to host-derived nutrients versus the cost of host cell turnover and exposure to the inflammatory mediators of the host immune response. Microbes typically solve this dilemma by expressing adhesins for targeted adherence using a homing mechanism often referred to as tissue tropism. Although the functional interpretation of such glycan−protein interactions has been described for several microbial pathogens, detailed understanding of the underlying biochemistry is difficult. This complexity stems primarily from low-affinity binding, and in particular so because the binding affinity of most adhesins for monosaccharides is exceedingly low, in the millimolar range, whereas the binding affinity for complex glycans is in the 1−10 μM range. Hence, for biological events, multivalent binding often amplifies the relatively low-affinity binding to glycans,[15] a phenomenon best illustrated by binding to heavily glycosylated mucin molecules. Similarly, microbes gain binding strength by multivalent presentation of their adhesive subunits,

dx.doi.org/10.1021/ac201260c |*Anal. Chem.* XXXX, XXX, 000–000

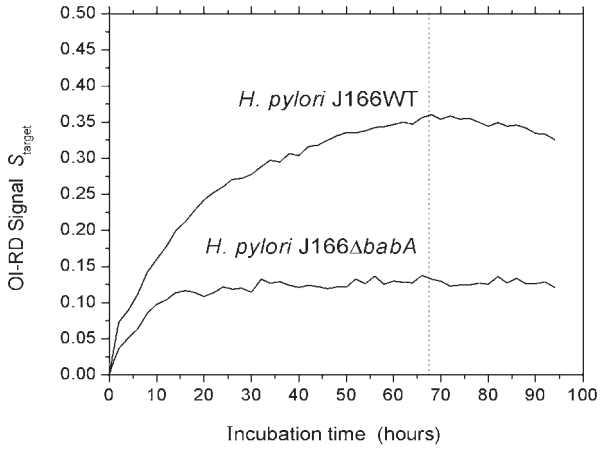

Figure 5. Whole bacterial cells exhibit slow binding kinetics. J166WT binding leveled off after 66 h, whereas J166Δ*babA* mutant binding was faster and leveled off after only 15 h of incubation. The diagrams depict the association−dissociation curves of J166WT and J166Δ*babA* with immobilized Le^b−HSA. The dashed line marks the time at which 1× PBS (buffer) replaces the bacterial solution in the fluidic chamber and the time at which the images shown in Figure 3 were obtained.

often displaying hundreds of glycan-binding pili or toxins. Examples include the cholera toxin that binds sialylated GM1-glycan in the intestine[16] and the hemagglutinin molecules on the surface of influenza A virus that bind to sialylated carbohydrates. The importance of low-affinity binding has stimulated strategies for assays based on multivalency in receptor presentation.[17−19]

In the present study, we investigated binding to surface-presented blood group antigens by the gastric pathogen, *H. pylori*. Binding analyses of soluble blood group antigens under conditions of equilibrium have shown that high-affinity binding of *H. pylori* is mediated by BabA.[12,20] Further, *H. pylori* strains that express BabA are isolated more frequently from individuals with peptic ulcers or gastric cancer,[21] suggesting that tight mucosal binding is a risk factor for development of overt disease. However, BabA expression is often lost during infection in animal models,[22,23] which implies that *H. pylori* has complementary adhesins with lower binding affinities that make them difficult to detect.

One such low-affinity adhesin is SabA, which mediates binding to sialylated antigens.[14] During *H. pylori* infection, the predominantly fucosylated mucosal glycosylation shifts to more sialylated patterns.[14,24] The SabA adhesin binds to the sialylated mucosal landscape, though with 100-fold lower affinity compared to BabA binding to ABO/Le^b. To investigate the presence of a second line of attachment proteins complementary to BabA but with substantially lower binding affinities, we used a solid-phase whole-cell binding assay that takes advantage of the "Velcro effect" of multivalent presentation of receptors. Of particular relevance, ligand presentation is important for interpretation of biological receptor activities. For example, *H. pylori* binds with similar affinity to a series of free fucosylated oligosaccharides (glycans) such as H-1, H-2, Le^b, and Le^y (i.e., mono- vs difucosylated structures) based on either the lacto-series type-1 or type-2 core chains. However, when these glycans are covalently attached to a carrier to make multivalent glycoconjugates, the bacterial affinity for H-1 and Le^b increases >1000-fold, whereas the affinity for H-2, Le^a, Le^x, and Le^y is completely lost.[20] *H. pylori babA* deletion mutants do not bind soluble Le^b conjugates,[12,20] which argues that complementary adhesins may bind the ABO/Le^b antigens with affinities that are reduced several log-fold. This discrepancy necessitates development of techniques for more sensitive detection and visualization of the binding activity of intact bacterial cells.

In this report we present a novel experimental platform based on a combination of solid-phase immobilized glycoconjugates and OI-RD microscopy for real-time detection of *H. pylori* whole-cell binding. On this platform, *H. pylori* binds with high strength to Le^b blood group antigens but not to the closely related Le^a, Le^x, or Le^y antigens (Figures 3 and 4). This specificity is in complete agreement with previous studies on *H. pylori* binding to soluble glycoconjugates. Furthermore, the specificity in binding to the Le^b antigen but not to Le^a, Le^x, or Le^y antigens was reproduced using recombinant BabA protein (Figure 2 and Supporting Information Figure S3). Surprisingly OI-RD microscopy revealed that *babA* deletion mutants also bind to Le^b antigen with high specificity, albeit with lower binding strength (Figures 3 and 4). The residual lower-affinity Le^b binding properties have escaped previous detection using assays based on soluble adhesin−glycan interactions. This label-free solid-phase binding assay platform is particularly useful for study of these cells, as most *H. pylori* outer-membrane proteins demonstrate high isoelectric points (pI); hence, many labeling reagents react readily with basic charged amino acids that might sterically inhibit binding. Furthermore, OI-RD microscopy can be used in real time to analyze simultaneous binding of intact microorganisms to thousands of receptors. The increased sensitivity, high throughput, and real-time analysis of whole bacterial cell binding to multivalent receptors in solid-supported microarray format may permit identification of discrete attachment mechanisms essential for infectious processes and perhaps, in turn, could identify novel targets for drug or vaccine development.

■ ASSOCIATED CONTENT

Supporting Information. Additional information as noted in text. This material is available free of charge via the Internet at http://pubs.acs.org.

■ AUTHOR INFORMATION

Corresponding Author

*E-mail: Thomas.Boren@medchem.umu.se (T.B.); xdzhu@physics.ucdavis.edu (X.D.Z.).

■ ACKNOWLEDGMENT

This study was supported by Grants to T.B. from the Swedish Research Council (Grant No. 11218), the Swedish Cancer Foundations, and the J. C. Kempe and Seth M. Kempe Memorial Foundation, to J.V.S. from the National Institutes of Health (R01 AI070803, R01 AI081037), and to X.D.Z. from the National Institutes of Health (R01 HG003827-04, R01 GM076360-04S1). We thank Prof. Dr. Stefan Dübel (Technical University of Braunschweig, Germany) for providing the bacterial expression vector pOPE101.

■ REFERENCES

(1) Paulson, J. C.; Blixt, O.; Collins, B. E. *Nat. Chem. Biol.* **2006**, *2*, 238–248.

(2) Liang, P. H.; Wu, C. Y.; Greenberg, W. A.; Wong, C. H. *Curr. Opin. Chem. Biol.* **2008**, *12*, 86–92.

(3) Landry, J. P.; Zhu, X. D.; Gregg, J. *Opt. Lett.* **2004**, *29*, 581–583.
(4) Zhu, X. D.; Landry, J. P.; Sun, Y. S.; Gregg, J. P.; Lam, K. S.; Guo, X. W. *Appl. Opt.* **2007**, *46*, 1890–1895.
(5) Landry, J. P.; Sun, Y. S.; Guo, X. W.; Zhu, X. D. *Appl. Opt.* **2008**, *47*, 3275–3288.
(6) Fei, Y. Y.; Landry, J. P.; Sun, Y. S.; Zhu, X. D.; Luo, J. T.; Wang, X. B.; Lam, K. S. *Rev. Sci. Instrum.* **2008**, *79*, 013708.
(7) Sun, Y. S.; Landry, J. P.; Fei, Y. Y.; Zhu, X. D.; Luo, J. T.; Wang, X. B.; Lam, K. S. *Langmuir* **2008**, *24*, 13399–13405.
(8) Sun, Y. S.; Landry, J. P.; Fei, Y. Y.; Zhu, X. D.; Luo, J. T.; Wang, X. B.; Lam, K. S. *Anal. Chem.* **2009**, *81*, 5373–5380.
(9) Fei, Y. Y.; Landry, J. P.; Sun, Y. S.; Zhu, X. D.; Wang, X. B.; Wu, C. Y.; Lam, K. S. *J. Biomed. Opt.* **2010**, *15*, 016018.
(10) Kusters, J. G.; van Vliet, A. H.; Kuipers, E. J. *Clin. Microbiol. Rev.* **2006**, *19*, 449–490.
(11) Borén, T.; Falk, P.; Roth, K. A.; Larson, G.; Normark, S. *Science* **1993**, *262*, 1892–1895.
(12) Aspholm-Hurtig, M.; Dailide, G.; Lahmann, M.; Kalia, A.; Ilver, D.; Ilver, D.; Roche, N.; Vikström, S.; Sjöström, R.; Lindén, S.; Bäckström, A.; Lundberg, C.; Arnqvist, A.; Mahdavi, J.; Nilsson, U. J.; Velapatino, B.; Gilman, R. H.; Gerhard, M.; Alarcon, T.; Lopez-Brea, M.; Nakazawa, T.; Fox, J. G.; Correa, P.; Dominguez-Bello, M. G.; Perez-Perez, G. I.; Blaser, M. J.; Normark, S.; Carlstedt, I.; Oscarson, S.; Teneberg, S.; Berg, D. E.; Borén, T. *Science* **2004**, *305*, 519–522.
(13) Alm, R. A.; Bina, J.; Andrews, B. M.; Doig, P.; Hancock, R. E.; Trust, T. J. *Infect. Immun.* **2000**, *68*, 4155–4168.
(14) Mahdavi, J.; Sondén, B.; Hurtig, M.; Olfat, F. O.; Forsberg, L.; Roche, N.; Ångstrom, J.; Larsson, T.; Teneberg, S.; Karlsson, K. A.; Altraja, S.; Wadström, T.; Kersulyte, D.; Berg, D. E.; Dubois, A.; Petersson, C.; Magnusson, K. E.; Norberg, T.; Lindh, F.; Lundskog, B. B.; Arnqvist, A.; Hammarström, L.; Borén, T. *Science* **2002**, *297*, 573–578.
(15) Adler, P.; Wood, S. J.; Lee, Y. C.; Lee, R. T.; Petri, W. A., Jr.; Schnaar, R. L. *J. Biol. Chem.* **1995**, *270*, 5164–5171.
(16) Holmgren, J.; Lönnroth, I.; Månsson, J.; Svennerholm, L. *Proc. Natl. Acad. Sci. U.S.A.* **1975**, *72*, 2520–2524.
(17) Borén, T.; Normark, S.; Falk, P. *Trends Microbiol.* **1994**, *2*, 221–228.
(18) Falk, P.; Borén, T.; Normark, S. *Methods Enzymol.* **1994**, *236*, 353–374.
(19) Aspholm, M.; Kalia, A.; Ruhl, S.; Schedin, S.; Arnqvist, A.; Lindén, S.; Sjöström, R.; Gerhard, M.; Semino-Mora, C.; Dubois, A.; Unemo, M.; Danielsson, D.; Teneberg, S.; Lee, W. K.; Berg, D. E.; Borén, T. *Methods Enzymol.* **2006**, *417*, 293–339.
(20) Ilver, D.; Arnqvist, A.; Ögren, J.; Frick, I. M.; Kersulyte, D.; Rad, R.; Incecik, E. T.; Berg, D. E.; Covacci, A.; Engstrand, L.; Borén, T. *Science* **1998**, *279*, 373–377.
(21) Gerhard, M.; Lehn, N.; Neumayer, N.; Borén, T.; Rad, R.; Schepp, W.; Miehlke, S.; Classen, M.; Prinz, C. *Proc. Natl. Acad. Sci. U.S.A.* **1999**, *96*, 12778–12783.
(22) Solnick, J. V.; Hansen, L. M.; Salama, N. R.; Boonjakuakul, J. K.; Syvanen, M. *Proc. Natl. Acad. Sci. U.S.A.* **2004**, *101*, 2106–2111.
(23) Styer, C. M.; Hansen, L. M.; Cooke, C. L.; Gundersen, A. M.; Choi, S. S.; Berg, D. E.; Benghezal, M.; Marshall, B. J.; Peek, R. M., Jr.; Borén, T.; Solnick, J. V. *Infect. Immun.* **2010**, *78*, 1593–1600.
(24) Lindén, S.; Mahdavi, J.; Semino-Mora, C.; Olsen, C.; Carlstedt, I.; Borén, T.; Dubois, A. *PLoS Pathog.* **2008**, *4*, e2.
(25) Solnick, J. V.; Hansen, L. M.; Canfield, D. R.; Parsonnet, J. *Infect. Immun.* **2001**, *69*, 6887–6892.